Research Square

Preprints are preliminary reports that have not undergone peer review.
They should not be considered conclusive, used to inform clinical practice,
or referenced by the media as validated information.

Mineral-Specific Iron Oxidation States and Oxygen Fugacity of Mantle Xenoliths from Jeju and Baengnyeong Islands

Mi-Eun Jin
Korea Atomic Energy Research Institute
Young Rang Uhm
uyrang@kaeri.re.kr

Korea Atomic Energy Research Institute
Gwang-Min Sun
Korea Atomic Energy Research Institute
Yong-Joo Jwa
Gyeongsang National University
Dong Hyeok Moon
Korea Institute of Geoscience and Mineral Resources
Hang-Jae Lee
Korea Institute of Geoscience and Mineral Resources

Research Article

Keywords: Basalt, Spinel lherzolite, Mössbauer spectroscopy, Iron oxidation state, Oxygen fugacity

Posted Date: November 13th, 2026

DOI: https://doi.org/10.21203/rs.3.rs-11550829/v1

License: This work is licensed under a Creative Commons Attribution 4.0 International License.
Read Full License

Additional Declarations: No competing interests reported.

Mineral-Specific Iron Oxidation States and Oxygen Fugacity of Mantle Xenoliths from Jeju and Baengnyeong Islands

Mi-Eun Jin[1], Young Rang Uhm[1*], Gwang-Min Sun[1], Yong-Joo Jwa[2], Dong Hyeok Moon[3], Hang-Jae Lee[3]

[1]*HANARO Utilization Division, Korea Atomic Energy Research Institute, Daejeon, 34057, South Korea*

[2]*Department of Geology, Gyeongsang National University, Jinju, 52828, South Korea*

[3] *Korea Institute of Geoscience and Mineral Resources, Deajeon, 34132, South Korea*

*Corresponding Author: uyrang@kaeri.re.kr

Abstract

This study investigated the iron oxidation states and redox characteristics of spinel lherzolite xenoliths from Jeju and Baengnyeong Islands, South Korea, using electron probe microanalysis (EPMA) and Mössbauer spectroscopy. Mössbauer spectroscopy was used to characterize the Fe^{2+} and Fe^{3+} distributions in individual minerals and determine the $Fe^{3+}/\Sigma Fe$ ratios in spinel, while EPMA provided the mineral compositions required for oxygen fugacity calculations. The calculated oxygen fugacity values ranged from -0.84 to -0.12 log units relative to the fayalite–magnetite–quartz (FMQ) buffer, revealing differences in redox conditions among the investigated samples. These findings provide

insights into the mineral-specific iron oxidation states and redox characteristics of mantle xenoliths from the two regions.

Keywords

Basalt, Spinel lherzolite, Mössbauer spectroscopy, Iron oxidation state, Oxygen fugacity

Introduction

The oxidation states of iron in geological materials provide important information about physicochemical conditions and redox environments associated with rock formation and evolution. In particular, the distribution of Fe^{2+} and Fe^{3+} in minerals is closely related to oxygen fugacity (fO_2), which is a key parameter for understanding magmatic processes and the oxidation state of the Earth's interior [1–2]. Mantle xenoliths are fragments of upper-mantle rocks transported to the Earth's surface by ascending basaltic magmas. Because they preserve mineralogical and geochemical information about the mantle, they provide valuable insights into upper-mantle composition, heterogeneity, and magmatic evolution [3]. The iron oxidation states of their constituent minerals are particularly important because they reflect redox conditions influenced by processes such as partial melting, mantle–melt interaction, and metasomatism [4–7]. Consequently, investigating the distribution of Fe^{2+} and Fe^{3+} among individual mantle minerals is essential for evaluating the redox characteristics of mantle-derived rocks.

Several analytical techniques are available for investigating iron oxidation states, including electron probe microanalysis (EPMA), wet-chemical analysis, X-ray absorption spectroscopy (XAS), and Mössbauer spectroscopy. EPMA provides quantitative mineral compositions and total iron concentrations with high spatial resolution. However, conventional EPMA does not directly distinguish Fe^{2+} from Fe^{3+}, and their proportions are generally inferred from mineral stoichiometry and charge-balance calculations [8]. In contrast, Mössbauer spectroscopy provides information on iron oxidation states, local coordination environments, and magnetic properties through the hyperfine interactions of

^{57}Fe nuclei. The combination of these techniques therefore offers a complementary approach to characterizing iron-bearing minerals and evaluating their redox characteristics [9–10].

Previous studies in Korea have applied Mössbauer spectroscopy to volcanic rocks from Jeju Island [11–14], including investigations of alkali basalts and mantle xenoliths [15]. However, comparative studies of the iron oxidation states of individual minerals in mantle xenoliths from different Korean volcanic regions remain limited. Spinel is particularly important in this context because its $Fe^{3+}/\Sigma Fe$ ratio, combined with the chemical compositions of coexisting minerals, can be used to calculate oxygen fugacity. Previous studies have demonstrated the application of Mössbauer spectroscopy to determining the $Fe^{3+}/\Sigma Fe$ ratios of spinel and evaluating mantle redox conditions using mineral equilibria [16–17].

In this study, basalts and spinel lherzolite xenoliths from Jeju and Baengnyeong Islands, South Korea, were investigated using EPMA and Mössbauer spectroscopy. The iron oxidation states of the constituent minerals, including olivine, orthopyroxene, clinopyroxene, and spinel, were characterized and compared. In particular, the $Fe^{3+}/\Sigma Fe$ ratios of spinel determined by Mössbauer spectroscopy were combined with EPMA-derived mineral compositions to calculate oxygen fugacity. The objective was to compare the mineral-specific iron oxidation states and evaluate variations in the redox characteristics of mantle xenoliths from the investigated regions.

Sample Preparation and Experimental Methods

The Korean Peninsula is located within the Eurasian Plate, in a tectonic setting influenced by the subduction of the Philippine Sea Plate and the Pacific Plate beneath the Eurasian Plate. On Jeju Island and Baengnyeong Island, ultramafic mantle xenoliths derived from the upper mantle occur in small volumes within alkali basalts [18–19]. Various types of mantle-derived xenoliths have been reported from the alkali basalts of Jeju and Baengnyeong Islands, including spinel peridotites, pyroxenites, gabbroic xenoliths, and

clinopyroxene megacrysts [19–21]. The mantle xenoliths reported from these regions are predominantly classified as spinel lherzolites [8, 20–21]. As the xenoliths investigated in this study also belong to this group, they are hereafter referred to as spinel lherzolites. The samples used in this study comprise basalts and spinel lherzolites collected from the Gyorae-ri area (JG-1b and JG-1x) and the Sinsan-ri area (1FAF-6b, 1FAF-14b, 1FAF-6x, and 1FAF-14x) on Jeju Island, as well as spinel lherzolites from Baengnyeong Island, Incheon (1FAF-1x) (**Fig. 1a, b**). Some of the studied rock specimens were housed at the Geological Museum, KIGAM (e.g., 1FAF-1, 6, 14). To characterize the magnetic properties of the constituent minerals, the minerals in the spinel lherzolites were individually separated and prepared. Wherever possible, sample portions unaffected by surface weathering were selected for analysis. These relatively fresh portions were considered to preserve the original characteristics of the spinel lherzolites more effectively and thus provide a more reliable representation of the geochemical characteristics of the upper mantle. In addition, basalt samples devoid of spinel lherzolite xenoliths from the Gamsan-ri area of Jeju Island (JG-4b) were analyzed to compare their oxidation states with those of xenolith-bearing basalts (**Table 1**).

Electron probe microanalysis (EPMA) was performed to determine the geochemical compositions of the major constituent minerals of the spinel lherzolites. The analyzed minerals included olivine, orthopyroxene, clinopyroxene, and spinel. Analyses were conducted using a field-emission electron probe microanalyzer (FE-EPMA, JXA-110 iHP200F, JEOL) at an accelerating voltage of 15 kV, a beam current of 20 nA, and an electron beam diameter of 1 μm.

Mössbauer spectroscopy was performed to investigate the oxidation states and crystallographic environments of iron within the samples. Measurements were conducted on the host basalts and individual minerals separated from the spinel lherzolites. Transmission Mössbauer spectra were acquired at room temperature (290 K) using a ^{57}Co/Rh source with an 50 mCi manufactured by RITVERC Co. The spectra were calibrated using an α-^{57}Fe foil and fitted using MossWinn 4.0 software. For the basalts, the bulk iron oxidation state was investigated using whole-rock samples, whereas the spectra of each mineral from the spinel lherzolites were analyzed to compare the characteristics of Fe^{2+} and Fe^{3+}.

Results and discussion

Geochemical Composition

The major mineral assemblage of the spinel lherzolites consists of olivine, clinopyroxene, orthopyroxene, and Cr-bearing spinel. The spinel Cr-number (Cr# = $Cr^{3+}/(Cr^{3+} + Al^{3+}) \times 100$) is relatively low, with average values ranging from 10.67 to 24.80, while the average Al_2O_3 concentration of orthopyroxene ranges from 2.53 to 4.47 wt.%. These are consistent with the classification of the samples as Al-spinel lherzolites [22].

The EPMA results indicate that the spinel lherzolites from Jeju and Baengnyeong Island exhibit generally similar mineral chemical compositions. Olivine is predominantly classified as forsterite (Fo), with Fo values ranging from approximately Fo89 to Fo92 (Fig. 2a, Table 2), indicating Mg-rich olivine in the spinel lherzolites from both regions. Spinel compositions plot within the Fe-spinel field (Fig. 2b). The average Cr# values are 14.35 and 10.67 for Gyorae-ri and Sinsan-ri on Jeju Island, respectively, and 24.80 for Baengnyeong Island. Thus, spinel from Baengnyeong Island exhibits a higher Cr# than spinel from Jeju Island (Table 2).

Orthopyroxene is classified as Mg-rich enstatite, with composition ranging from $Wo_{0.67–1.39}$, $En_{89.2–91.6}$, and $Fs_{7.53–9.0}$(**Fig. 2c, Table 3**). Clinopyroxene is classified as Ca-rich diopside, with compositions ranging from $Wo_{45.1–46.4}$, $En_{48.7–50.9}$, and $Fs_{3.8–5.4}$ (**Fig. 2d, Table 3**). Overall, these results indicate that the investigated spinel lherzolites have broadly similar mineral assemblages and chemical compositions, although variations in spinel Cr# may reflect differences in the degree of partial melting or mantle depletion.

Mössbauer Spectroscopy

The Mössbauer spectra of the basalts 1FAF-6b, 1FAF-14b, and JG-4b, as well as those of the individual minerals separated from the spinel lherzolites, are presented in **Fig. 3** and **4.** The hyperfine parameters obtained through spectral fitting are listed in **Table 4-6**. Data for

JG-1b were taken from [15].

The Mössbauer spectra of the basalts were fitted with two doublets attributed to Fe^{2+} in olivine and clinopyroxene, together with one doublet attributed to Fe^{3+}. The Fe^{2+} doublets, with isomer shift (IS) values of 1.04–1.12 mm/s and quadrupole splitting (QS) values of 2.90–2.91 mm/s, are characteristic of olivine [15, 23-24]. The dominant Fe^{2+} doublets, with IS values of 0.75–1.03 mm/s and QS values of 2.04–2.55 mm/s (**Table 4**) are assigned to clinopyroxene [23].

In contrast, JG-4b, a basalt sample without spinel lherzolite xenoliths, exhibited additional magnetic components with hyperfine parameters attributed to magnetite, unlike the other basalt samples.

The $Fe^{3+}/\Sigma Fe$ ratios of JG-1b, 1FAF-6b and 1FAF-14b ranged from 19.40 to 31.08 %, whereas JG-4b exhibited a higher reported $Fe^{3+}/\Sigma Fe$ ratio of 42.24 % (**Table 4**).

These differences suggest variations in iron oxidation states and the occurrence of iron oxides among the basalt samples, potentially reflecting differences in their formation or subsequent alteration histories [25]. However, additional mineralogical and geochemical analyses are required to establish the origin of these variations and evaluate their relationship to formation conditions.

A notable feature of the Mössbauer spectra of the individual minerals separated from the spinel lherzolites is the absence of magnetic sextets. The olivine spectra were fitted with two doublets attributed to Fe^{2+}. Olivine, a major constituent mineral of mantle-derived rocks, is generally considered to contain negligible amounts of Fe^{3+} [26–30]. Accordingly, the Fe^{3+} contribution to the Mössbauer spectra of olivine was considered negligible in this study (**Table 5**).

The Mössbauer spectra of the pyroxene-group minerals, clinopyroxene and orthopyroxene, were generally fitted with doublets attributed to Fe^{2+} at the M1 site (QS = 2.89–3.00 mm/s; IS = 1.04–1.06 mm/s) and the M2a site (QS = 2.04–2.13 mm/s; IS = 1.03–1.06 mm/s), together with a doublet attributed to Fe^{3+} (QS = 0.39–0.69 mm/s; IS = 0.03–0.23 mm/s). In orthopyroxene, an additional Fe^{2+} component, designated M2b (QS = 2.23–2.26 mm/s; IS = 1.07–1.12 mm/s), was also observed (**Table 6**).

The $Fe^{3+}/\Sigma Fe$ ratios of orthopyroxene and clinopyroxene varied slightly among the investigated samples. Consistent with previous studies of spinel lherzolites, orthopyroxene

exhibited lower $Fe^{3+}/\Sigma Fe$ ratios than clinopyroxene [28, 30–33]. Specifically, the $Fe^{3+}/\Sigma Fe$ ratios ranged from 17.22 to 21.73% for clinopyroxene and from 7.94 to 11.46% for orthopyroxene (**Table 6**).

Both Fe^{2+} and Fe^{3+} were identified in spinel, with a relatively higher Fe^{3+} contribution than in the other investigated silicate minerals. The Mössbauer spectra of spinel were generally fitted with one doublet attributed to Fe^{3+} (QS = 0.28–0.68 mm/s; IS = 0.18–0.44 mm/s) and three doublets attributed to Fe^{2+}. The $Fe^{3+}/\Sigma Fe$ ratios of spinel ranged from 18.94 to 27.68%, exceeding those of orthopyroxene and overlapping with or exceeding those of clinopyroxene (**Table 5**).

Overall, the Mössbauer results demonstrate that the distribution of Fe^{2+} and Fe^{3+} varies among the constituent minerals of the spinel lherzolites. Mineral-specific characterization of iron oxidation states, combined with mineral chemical compositions, provides a basis for evaluating the redox characteristics of the investigated mantle xenoliths.

Estimation of Oxidation State

To evaluate the mantle origin of the spinel lherzolites and assess the preservation of their primary mineral compositions, the Cr/(Cr + Al) atomic ratios of spinel were plotted against the forsterite (Fo) values of coexisting olivine [19–20, 34–35]. The samples plot within the Olivine-Spinel Mantle Array (OSMA), supporting their mantle origin and indicating that their olivine–spinel compositions are consistent with those of mantle peridotites (Fig. 6).

In this study, oxygen fugacity was calculated to quantitatively compare the redox conditions of the spinel lherzolites. Previous studies reported temperatures of 882-1038 °C and an average pressure of 17.7 kbar for spinel lherzolites from Jeju Island [8, 20], and temperatures of 897-1060 °C and a pressure of 16 kbar for spinel lherzolites from Boeun, Ganseong, and Baengnyeong Island [20, 36]. Because sample-specific temperature and pressure estimates were not available, representative conditions based on previous studies were adopted for the oxygen fugacity calculations: 1023 °C and 17 kbar for Jeju Island and 1007 °C and 15 kbar for Baengnyeong Island, respectively.

The magnetite activity in spinel and oxygen fugacity were calculated using the equations reported in Ref. [16]. In that study, the $Fe^{3+}/\Sigma Fe$ ratios of spinel in spinel lherzolites were determined using ^{57}Fe Mössbauer spectroscopy, and oxygen fugacity was calculated based on olivine–orthopyroxene–spinel equilibrium. The calculation incorporates the Fe^{2+} and Fe^{3+} compositions of spinel, the mole fractions of Fe and Mg in the relevant coexisting minerals, and temperature and pressure.

Using the spinel $Fe^{3+}/\Sigma Fe$ ratios determined by Mössbauer spectroscopy together with the EPMA-derived mineral compositions, the calculated $\Delta \log fO_2$ values relative to the fayalite–magnetite–quartz (FMQ) buffer were approximately −0.12 for JG-1x, −0.84 for 1FAF-6x, and −0.66 for 1FAF-1x. Among the investigated samples, JG-1x exhibited the highest oxygen fugacity, whereas 1FAF-6x and 1FAF-1x showed relatively lower values. Although all samples yielded oxygen fugacity values below the FMQ buffer-suggesting relatively reduced environments-JG-1x exhibits a relatively more oxidized state than the other samples.

Previous studies reported $\Delta \log fO2$ values of approximately -1.5 to -0.5 for spinel lherzolites from Baengnyeong Island and -1.1 to +0.4 for those from Jeju Island [8, 21, 37, 38]. The values calculated in this study fall within these previously reported ranges (Fig. 7), indicating that the investigated spinel lherzolites exhibit redox characteristics consistent with those previously reported for mantle xenoliths from these regions.

An important aspect of this study is the characterization of mineral-specific iron oxidation states using Mössbauer spectroscopy. Olivine and pyroxenes predominantly contain Fe^{2+}, whereas spinel exhibits a relatively higher Fe^{3+} contribution. The $Fe^{3+}/\Sigma Fe$ ratios of spinel, combined with the chemical compositions of coexisting minerals determined by EPMA, provide the basis for evaluating oxygen fugacity. Overall, the results demonstrate differences in the calculated redox conditions among the investigated mantle xenoliths and highlight the complementary roles of Mössbauer spectroscopy and EPMA in characterizing mantle-derived geological materials.

Conclusions

In this study, the mineral chemical compositions and iron oxidation states of basalts and spinel lherzolite xenoliths from Jeju and Baengnyeong Islands were investigated using

EPMA and Mössbauer spectroscopy. The $Fe^{3+}/\Sigma Fe$ ratios of spinel were combined with the chemical compositions of coexisting minerals to calculate oxygen fugacity and compare the redox characteristics of the investigated mantle xenoliths.

EPMA results showed that the spinel lherzolites from both regions consist mainly of olivine, orthopyroxene, clinopyroxene, and spinel, with broadly similar mineral chemical compositions. Mössbauer spectroscopy revealed variations in iron oxidation states among the constituent minerals. Olivine and pyroxenes were dominated by Fe^{2+}, whereas spinel exhibited a relatively higher Fe^{3+} contribution.

The calculated oxygen fugacity values relative to the fayalite–magnetite–quartz (FMQ) buffer were -0.12 for JG-1x, -0.84 for 1FAF-6x, and -0.66 for 1FAF-1x. These values are consistent with previously reported ranges for mantle xenoliths from the two regions, while indicating differences in redox conditions among the investigated samples. The basalt samples also exhibited variations in Mössbauer spectral characteristics, including the occurrence of magnetite in JG-4b, suggesting differences in their iron-bearing mineral assemblages and oxidation states. However, further studies are required to determine whether these variations result from differences in the redox conditions during rock formation or from redox state modifications within the volcanic conduit near the surface. Overall, this study demonstrates that mineral-specific Mössbauer analysis, combined with EPMA-derived mineral compositions, provides a useful approach for comparing iron oxidation states and evaluating the redox characteristics of mantle xenoliths.

Acknowledgements

This study was supported by the Korea Atomic Energy Research Institute (KAERI) grant fund from the Korean government (MSIT) (No. 1711078081) and the Basic Research Project Research on the development and dissemination of contents responding to public demand and social issues in geoscience (Project No. GP2025-001) of the Korea Institute of Geoscience and Mineral Resources (KIGAM). This study was also presented at the International Conference on Nuclear Analytical Techniques in 2026 (NAT2026), which was held in Seoul, Korea, from Sep. 6 to 10, 2026.

Declarations

Conflict of interest The authors declared that they have no known competing fnancial interests or personal relationships that could have appeared to infuence the work reported in this paper.

References

1. Xu Y, Menzies A, Vroon P, Mercier C, Lin (1998) Texture–Temperature–Geochemistry Relationships in the Upper Mantle as Revealed from Spinel Peridotite Xenoliths from Wangqing, NE China. J Petr 39:469-493
2. Hidas K, Falus G, Szabó C, Szabó P, Kovács I, Földes T (2007) Geodynamic implications of flattened tabular equigranular textured peridotites from the Bakony-Balaton Highland Volcanic Field (Western Hungary). J Geodyna 43:484-503
3. Kushiro I, Yoder H, Mysen B (1976) Viscosities of basalt and andesite melts at high pressures. J Geophy Res 81:1351-6356
4. Dyar M, David G, Martha W, Christopher A, Elizabeth C (2006) MÖSSBAUER SPECTROSCOPY OF EARTH AND PLANETARY MATERIALS. Annual Review of Earth and Palnetary Sciences 34:83-125
5. Frost D, McCammon C (2008) The Redox State of Earth's Mantle. Annual Review of Earth and Planetary Sciences 36:389-420
6. Arculus R (1985) Oxidation status of the mantle — past and present. Annual Review of Earth and Planetary Sciences 13:75-95
7. Hao X, Yi-Liang (2013) 57Fe Mössbauer spectroscopy of mineral assemblages in mantle spinel lherzolites from Cenozoic alkali basalt, eastern China: Petrological application. Lithos 156-159: 112-119
8. Choi S (2000) Oxidation of mantle xenoliths from jeju-do, South Korea. J Geosci 4:211-220
9. Mariola K, Marcin W, Joanna K (2022) High temperature transformation of iron-bearing minerals in basalt: Mössbauer spectroscopy studies. J Mineral 53:10–19

10. Goncharov A, Saltykova A (2008) Iron valency in minerals of xenoliths and redox state of the upper mantle (by Mössbauer spectroscopy data). Hype Interact 186:187–192
11. Hong S (1987) A Study on Mössbauer Effect of Iron State in the Volcanic Rock. J Cheju Nat'l Univ 24:53-65
12. Choi W, Ko J, Hong S (2004) Microscopic Study on Scoria of the eastern part of Jeju by XRD and Mössbauer Spectroscopy. J Cheju Nat'l Univ 17:89-94
13. Ko J, Yoon I (2017) A Study on Scoria at Older Cinder Cone in Jeju Island by Mössbauer Spectroscopy. J Korean Mag Soc 27:234-239
14. Ko J, Yoon I (2018) A Study on Mössbauer Spectroscopy of Scoria at the Younger Cinder Cone. J Korean Mag Soc 28 225-230
15. Jin M, Uhm Y, Sun G, Jwa Y (2025) A Mössbauer Study of Basalt and Mantle Xenolith in Jeju Island. J Korean Mag Soc 35:174-179
16. Ionov D, Wood B (1992) The oxidation state of subcontinental mantle: oxygen thermobarometry of mantle xenoliths from centeral Asia. Contri Mineral and Petrology. 111:179–193
17. Canil D, Oniell H, Pearson D, Rudnick R, Mcdonough W, Carswell D (1994) Ferric iron in peridotites and mantle oxidation states. Earth and Planetary Sci Lett 123:205-220
18. Kim K, Nagao K, Suzuki K, Tanaka T, Park E. (2003) Evidences of the presence of old continental basement in Jeju volcanic Island, South Korea, revealed by Radiometric ages and Nd-Sr isotopes of granitic rocks. J Geochem 36:421-441
19. Choi S (2012) Lithospheric Mantle beneath the Korean Peninsula: Implications from Peridotite Xenoliths in Alkali Basalts. J Korean Petrol Soc 21:235-247
20. Yun S, Koh J, Anh J (1998) A Study on the Spinel-Lherzolite Xenolith in the Alkali Basalt from Eastern Cheju Island, Korea. J Econ Environ Geol 31:447-458
21. Park G, Kim E, Kim S, Jeong H, Yang K. (2018) Petrology of peridotite xenoliths from the Neocene alkaline basalt From Baegryeong Island. J Korean Geol Soc 54:75-92
22. Carswell D (1980) Mantle derived lherzolite nodules associated with kimberlite, carbonatite and basaltic magmatism: a review. Lithos. 13:121-38

23. Stevens J, Khasanov A, Miller J, Pollak H, Li Z (2005). Mössbauer mineral handbook. Asheville, NC, USA: Mössbauer Effect Data Center, University of North Carolina.
24. Dariusz M, Martyna J, Jerzy Z, Artur B, Krzysztof R, Maria D (2017) Identification of iron-bearing minerals in basalts and pillow lavas of the Kaczawa Mountains using ^{57}Fe Mössbauer spectroscopy. J Nukleonika 62:145–148
25. Hammer J (2005) Influence of fO_2 and cooling rate on the kinetics and energetics of Fe-rich basalt crystallization. J Earth and Planetary Sci Let. 248(3-4):618-637
26. Nakamura A, Schmalzried H, (1983) On the stoichiometry and point defects of olivine. J Phys Chem of Mineral 10:27–37
27. O'Neill, H St C, Rubie, Canil D, Geiger D, Ross II, Seifert C, Woodland A, (1993) Ferric iron in the upper mantle and transition zone assemblages: implications for relative oxygen fugacities in the mantle. Evolution of the Earth and Planets. J Geophys Monogr 74:73–88
28. Canil D, O'Neill, HSt.C (1996) Distribution of ferric iron in some upper-mantle assemblages. J Petrology. 37:609–635
29. Woodland A, Angel R (2000) Phase relations in the system fayalite–magnetite at high pressures and temperatures. Contrib Mineral Petrol 139:734–747
30. Woodland A, Kornprobst J, Tabit A (2006) Ferric iron in orogenic lherzolite massifs and controls of oxygen fugacity in the upper mantle. Lithos. 89:222-241
31. Dyar M, McGuire A, Ziegler R (1989) Redox equilibria and crystal chemistry of coexisting minerals from spinel lherzolite mantle xenoliths. J American Mineral 74:969–980
32. McGuire A, Dyar M, Nielson J (1991) Metasomatic oxidation of upper mantle peridotite. Contrib Mineral Petrol 109:252–264
33. Luth R, Canil D (1993) Ferric iron in mantle-derived pyroxenes and a new oxybarometer for the mantle. J Contrib Mineral Petrol 113:236–248
34. Arai S (1987) An estimation of the least depleted spinel peridotite on the basis of olivine- spinel mantle array. Neues Jahrb Mineral Monatsh H8:347-354
35. Arai S (1994) Characterization of spinel peridotites by olivine-spinel compositional relationships: Review and interpretation. J Chem Geo 113:191-204

337 36. Lee H (1995) Petorchemical Study on the Mantle Xwnoliths in alkli basalts from S.
338 Korea: P-T Regime of Upper Mantle. J Korean Petro Soc 4:104-123
339 37. Woo Y, Yang K, Kil Y, Yun S, Arai S (2014) Silica- and LREE-enriched spinel
340 peridotite xenoliths from the Quaternary intraplate alkali basalt, Jeju Island, South
341 Korea: Old subarc fragments? Lithos. 208-209:312-323
342 38. Kim E, Park G, Kim S, Kil Y, Yang K (2017) Petrology and Geochemistry of
343 Peridotite Xenoliths from Miocene Alkaline Basalt Near the Mt. Baekdu Area. J
344 Korean Petro Soc 26(4):311-325
345

346 **Table 1**

347 List of sample names of the basalts and spinel lherzolite analyzed in this study

Sample name	JG-1	1FAF-6	1FAF-14	1FAF-1	JG-4
Sample location	Jeju, Gyoraeri	Jeju, Sinsanri		Inchon, Baengnyeongdo	Jeju, Gamsanri
		Sample provided by the Geological Museum, KIGAM			
Basalt	JG-1b	1FAF-6b	1FAF-14b	1FAF-1b	JG-4b
Spinel lherzolite	JG-1x	1FAF-6x	1FAF-14x	1FAF-1x	Not include
	Olivine, CPX, OPX, Spinel				

348

Table 2

Electron microprobe analysis of olivine and spinel in spinel lherzolites

Sample Name	JG-1x	1FAF-6x	1FAF-14x	1FAF-1x
		Olivine		
SiO_2	40.62	40.40	41.10	40.96
FeO(t)	9.53	10.03	8.24	8.67
MnO	0.14	0.14	0.12	0.13
MgO	50.00	49.74	51.05	50.36
CaO	0.04	0.05	0.05	0.06
Total	100.4	100.4	100.6	100.2
		Cations based on 4 oxygens		
Si	0.99	0.99	0.99	1.00
Fe(t)	0.19	0.21	0.16	0.18
Mn	0.00	0.00	0.00	0.00
Mg	1.82	1.81	1.84	1.83
Ca	0.00	0.00	0.00	0.00
Fe/Fe+Mg	0.10	0.10	0.08	0.09
Mg/Fe+Mg	0.90	0.90	0.92	0.91
		Spinel		
Al_2O_3	52.46	56.12		45.97
Cr_2O_3	13.10	9.99		22.60
FeO(t)	13.23	11.10		10.72
MnO	0.11	0.11		0.13
MgO	19.86	20.77		19.85
Total	99.22	98.58		99.65
		cations based on 4 oygens		
Al	1.64	1.73		1.47
Cr	0.27	0.21		0.48
Fe(t)	0.29	0.25		0.25
Mn	0.00	0.00		0.00
Mg	0.79	0.81		0.80
Cr#	14.35	10.67		24.80
Fe/Fe+Mg	27.19	23.06		23.24

352 **Table 3**

353 Electron microprobe analysis of orthopyroxene and clinopyroxene in spinel lherzolites

	Orthopyroxene				Clinopyroxene			
Sample Name	JG-1x	1FAF-6x	1FAF-14x	1FAF-1x	JG-1x	1FAF-6x	1FAF-14x	1FAF-1x
SiO_2	54.90	54.51	56.56	55.58	51.36	51.46	52.75	52.28
TiO_2	0.12	0.13	0.03	0.12	0.38	0.47	0.08	0.20
Al_2O_3	4.26	4.47	2.53	3.62	5.40	6.37	3.38	4.70
Cr_2O_3	0.47	0.34	0.63	0.54	0.80	0.82	1.51	1.15
FeO(t)	5.93	6.39	5.26	5.23	3.11	2.88	2.35	2.27
MnO	0.13	0.14	0.13	0.12	0.10	0.09	0.08	0.08
MgO	33.82	33.42	34.98	34.27	16.11	15.69	17.10	16.58
CaO	0.66	0.60	0.66	0.65	20.93	20.53	21.22	20.95
Na_2O	0.08	0.08	0.07	0.07	1.02	1.38	1.10	1.20
K_2O	0.01	0.01	0.01	0.00	0.00	0.02	0.00	0.00
Total	100.38	100.10	100.86	100.21	99.22	99.71	99.57	99.43
	Cations based on 6 oxygens							
Si	1.88	1.88	1.92	1.90	1.87	1.86	1.91	1.90
Ti	0.00	0.00	0.00	0.00	0.01	0.01	0.00	0.01
Al	0.12	0.12	0.08	0.10	0.13	0.14	0.09	0.10
Al	0.05	0.06	0.03	0.05	0.10	0.14	0.06	0.10
Cr	0.01	0.01	0.02	0.01	0.02	0.02	0.04	0.03
Fe(t)	0.17	0.19	0.15	0.15	0.09	0.09	0.07	0.07
Mn	0.00	0.00	0.00	0.00	0.00	0.00	0.00	0.00
Mg	1.73	1.71	1.77	1.75	0.88	0.85	0.92	0.90
Ca	0.02	0.02	0.02	0.02	0.82	0.80	0.82	0.81
Na	0.01	0.01	0.00	0.00	0.07	0.10	0.08	0.08
K	0.00	0.00	0.00	0.00	0.00	0.00	0.00	0.00
Wo	1.25	1.16	1.24	1.24	45.64	45.95	45.23	45.68
En	89.72	89.08	90.91	90.80	48.89	48.87	50.73	50.31
Fs	9.03	9.77	7.85	7.96	5.47	5.19	4.04	4.00

354

355

356 **Table 4**

357 Results of Mössbauer spectra for samples of basalt

		H_{hf}(kOe)	I.S.[mm/s]	Q.S. [mm/s]	Area [%]	Attributions
1FAF-6b	B1		0.38	0.69	23.16	Fe^{3+}
	B2		1.06	2.91	45.34	Ol (Fe^{2+})
	B3		0.81	2.55	31.50	CPX (Fe^{2+})
1FAF-14b	B1		0.70	1.15	31.08	Fe^{3+}
	B2		1.04	2.90	55.83	Ol (Fe^{2+})
	B3		0.75	2.46	13.09	CPX (Fe^{2+})
JG-4b	B1		0.47	0.63	17.96	Fe^{3+}
	B2		1.12	2.91	25.33	Ol (Fe^{2+})
	B3		1.03	2.04	18.78	CPX (Fe^{2+})
	MG1	473.3	0.80	0.09	13.64	MG O (Fe^{2+})
	MG2	492.8	0.23	-0.10	24.28	MG T (Fe^{3+})

358 H_{hf}(kOe) , Hyperfine Magnetic Field; IS, Isomer Shift; QS, Quadrupole Splitting; Ol, Olivine; CPX,

359 Clinopyroxene; MG O, Magnetite Octaheral; MG T, Magnetite Tetrahedral.

360 **Table 5**

361 Results of Mössbauer spectra for samples of olivine and spinel in spinel lherzolites

		I.S.[mm/s]	Q.S. [mm/s]	Area [%]	Attributions
Olivine					
JG-1x	Ol1	1.04	3.04	60.84	Fe^{2+}
	Ol2	1.01	2.86	39.16	Fe^{2+}
1FAF-6x	Ol1	0.87	2.72	77.33	Fe^{2+}
	Ol2	0.76	2.68	22.67	Fe^{2+}
1FAF-14x	Ol1	1.05	3.03	66.33	Fe^{2+}
	Ol2	0.89	2.89	33.67	Fe^{2+}
1FAF-1x	Ol1	1.08	3.01	77.12	Fe^{2+}
	Ol2	0.99	2.96	22.88	Fe^{2+}
Spinel					
JG-1x	S1	0.18	0.68	21.63	Fe^{3+}
	S2	0.79	1.29	37.67	Fe^{2+}
	S3	1.05	2.95	11.15	Fe^{2+}
	S4	0.86	1.99	29.56	Fe^{2+}
1FAF-6x	S1	0.20	0.60	27.68	Fe^{3+}
	S2	0.97	1.22	21.19	Fe^{2+}
	S2-1	0.78	1.34	33.51	Fe^{2+}
	S4	0.80	2.10	17.62	Fe^{2+}
1FAF-1x	S1	0.44	0.28	18.94	Fe^{3+}
	S2	0.65	1.47	27.76	Fe^{2+}
	S3	1.07	2.97	21.54	Fe^{2+}
	S4	0.85	1.87	31.76	Fe^{2+}

362

Table 6

Results of Mössbauer spectra for samples of clinopyroxene and orthopyroxene in spinel lherzolites

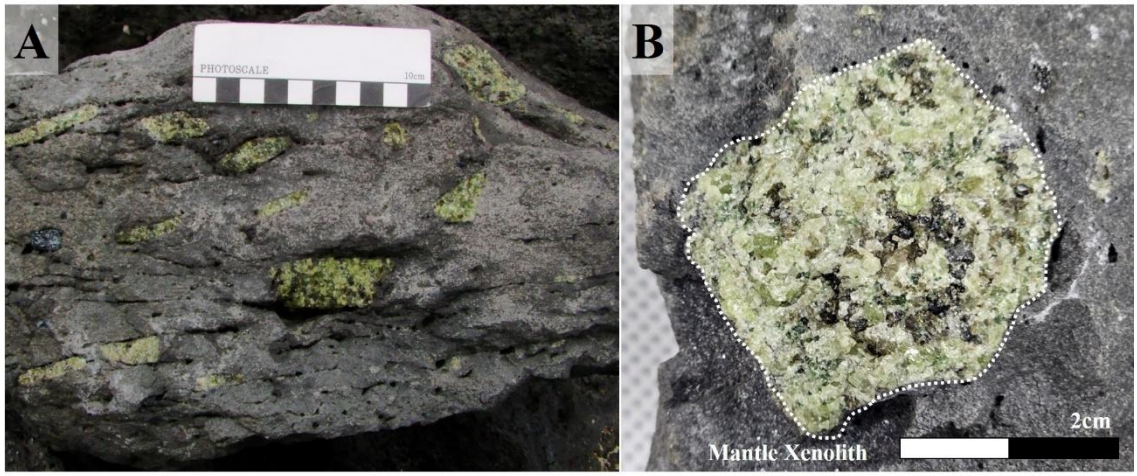
		IS[mm/s]	QS [mm/s]	Area [%]	Attributions
Clinopyroxene					
JG-1x	CP1	0.23	0.48	18.63	Fe^{3+}
	CP2	1.03	2.13	45.39	M2a(Fe^{2+})
	CP3	1.04	2.99	35.98	M1(Fe^{2+})
1FAF-6x	CP1	0.32	0.66	20.54	Fe^{3+}
	CP2	1.06	2.10	58.92	M2a(Fe^{2+})
	CP3	1.06	2.97	20.54	M1(Fe^{2+})
1FAF-14x	CP1	0.17	0.55	21.73	Fe^{3+}
	CP2	1.05	2.11	51.47	M2a(Fe^{2+})
	CP3	1.05	2.98	26.80	M1(Fe^{2+})
1FAF-1x	CP1	0.17	0.46	17.22	Fe^{3+}
	CP2	1.06	2.10	54.33	M2(Fe^{2+})
	CP3	1.06	3.00	33.45	M1(Fe^{2+})
Orthopyroxene					
JG-1x	OP1	0.03	0.69	11.46	Fe^{3+}
	OP2	1.03	2.09	37.55	M2a(Fe^{2+})
	OP3	1.07	2.99	19.83	M1(Fe^{2+})
	OP4	1.12	2.26	31.16	M2b(Fe^{2+})
1FAF-6x	OP1	0.06	0.49	7.94	Fe^{3+}
	OP2	1.05	2.17	67.85	M2a(Fe^{2+})
	OP3	1.08	3.04	14.32	M1(Fe^{2+})
	OP4	1.24	2.41	9.89	M2b(Fe^{2+})
1FAF-14x	OP1	0.07	0.39	9.71	Fe^{3+}
	OP2	1.04	2.12	52.09	M2a(Fe^{2+})
	OP3	1.05	2.99	15.95	M1(Fe^{2+})
	OP4	1.12	2.23	22.25	M2b(Fe^{2+})
1FAF-1x	OP1	0.11	0.49	11.05	Fe^{3+}
	OP2	1.04	2.04	29.51	M2a(Fe^{2+})
	OP3	1.06	2.99	29.36	M1(Fe^{2+})

	OP4	1.07	2.25	30.08	M2b(Fe^{2+})

366

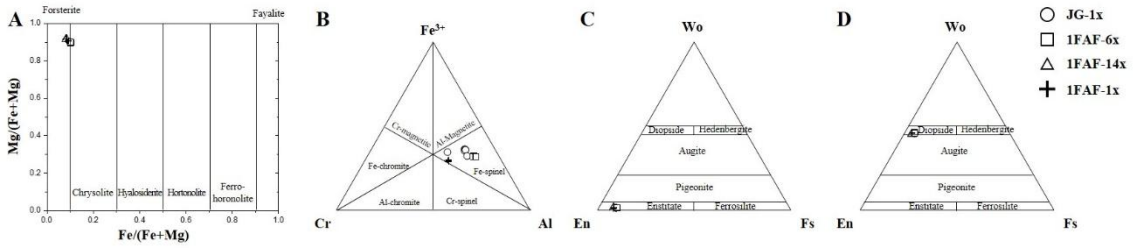
Fig. 1

Host basalts and spinel lherzolite xenoliths from the study areas (A) A spinel lherzolite included the host basalt (B) Spinel lherzolite



373 **Fig. 2**

374 Classification diagrams of spinel lherzolite (A) olivine (B) spinel (C)
375 orthopyroxene(enstatite) (D) clinopyroxene(diopside)

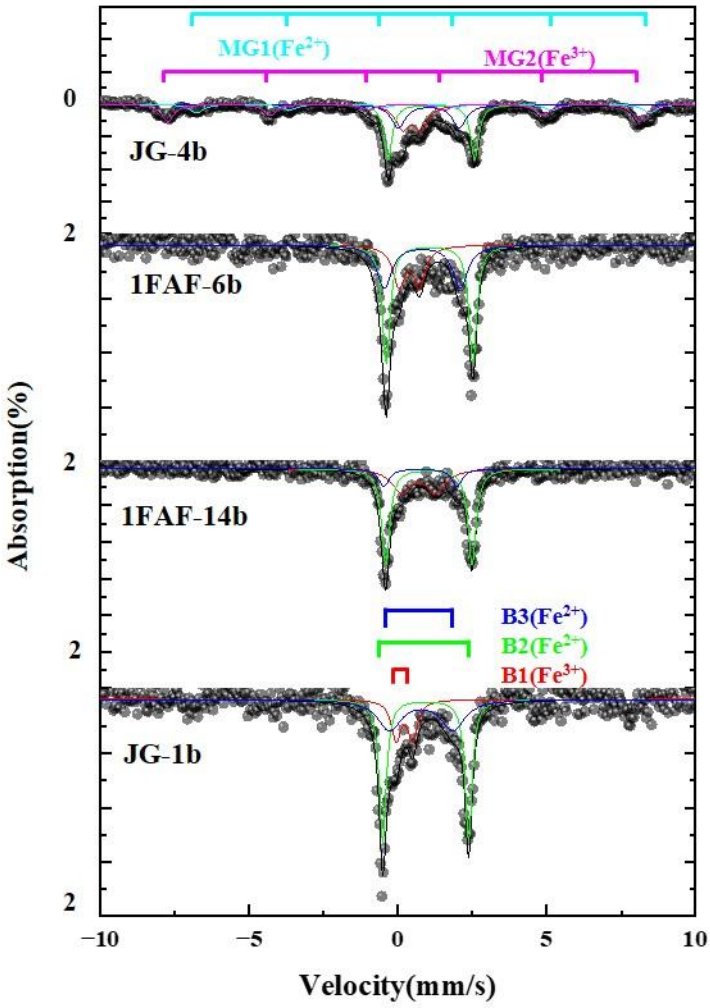


376

377 **Fig. 3**

378 The Mössbauer spectra for basalt on Jeju and Baengnyeong Island. Sample JG-1b was
379 reproduced and modified from [15]

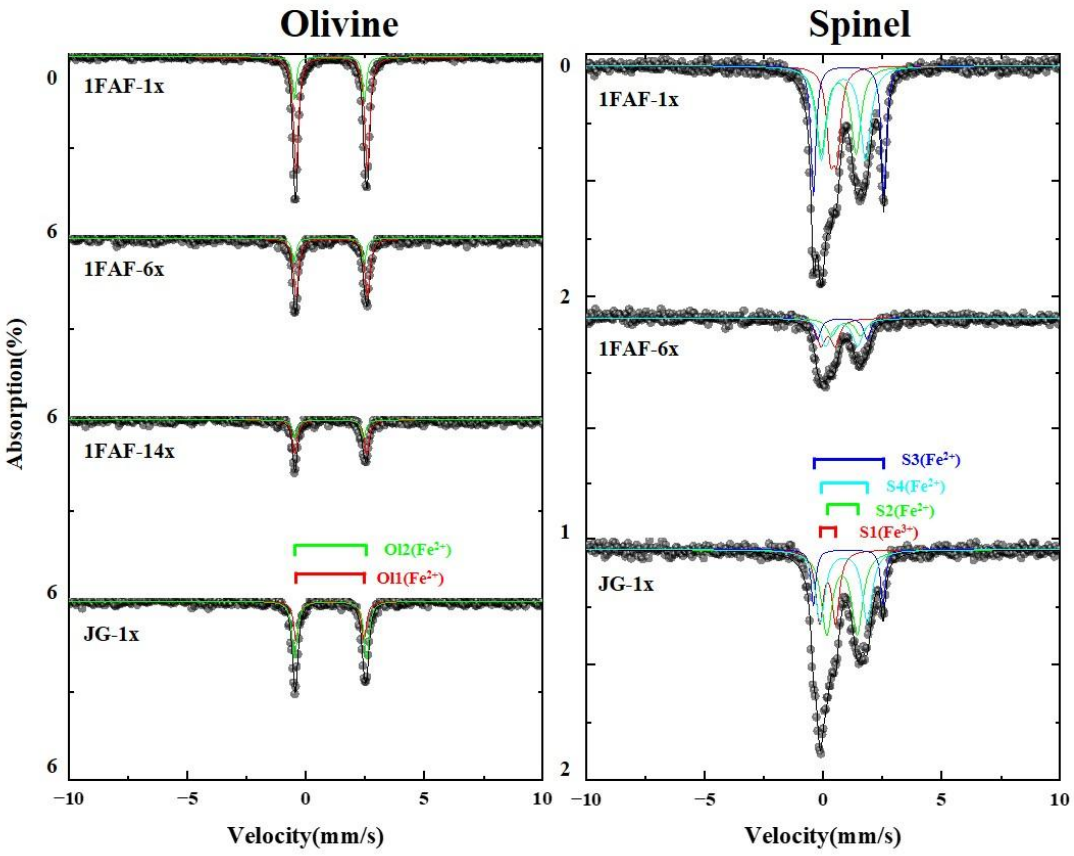
380



381

382 **Fig. 4**

383 The Mössbauer spectra for olivine and spinel of spinel lherzolites on Jeju and
384 Baengnyeong Island

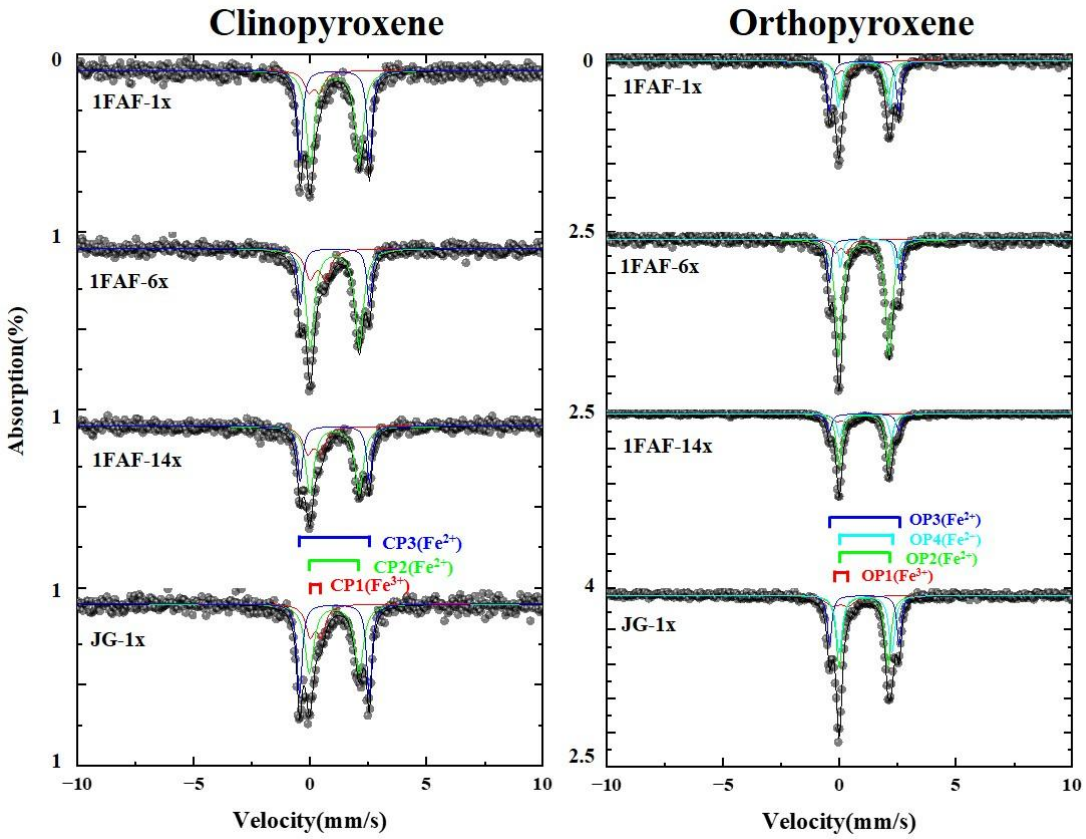


385

386

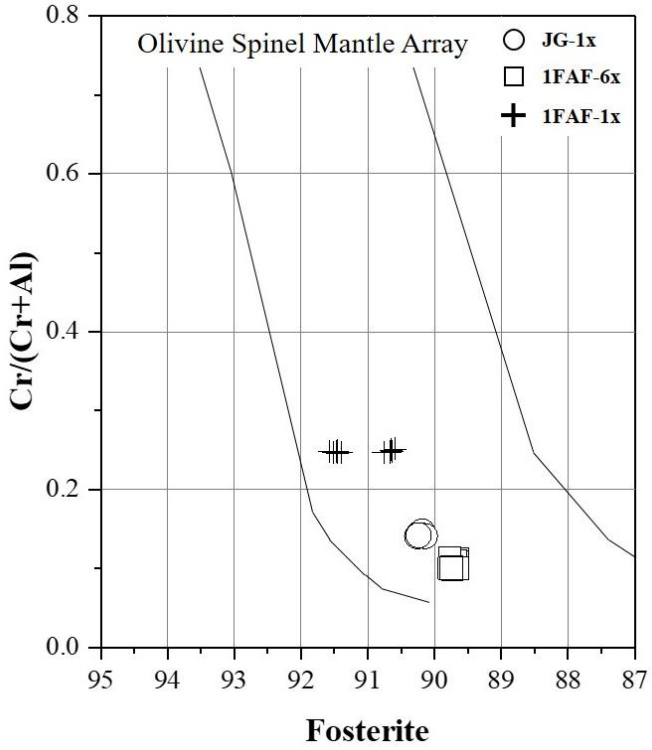
Fig. 5

The Mössbauer spectra for clinopyroxene and orthopyroxene of spinel lherzolites on Jeju and Baengnyeong Island.



392 **Fig. 6**

393 Cr/(Cr+Al) of spinel is plotted against Fosterite of coexisting olivine. The area is the
394 range of Olivine Spinel Mantel Array (after Arai, 1993)



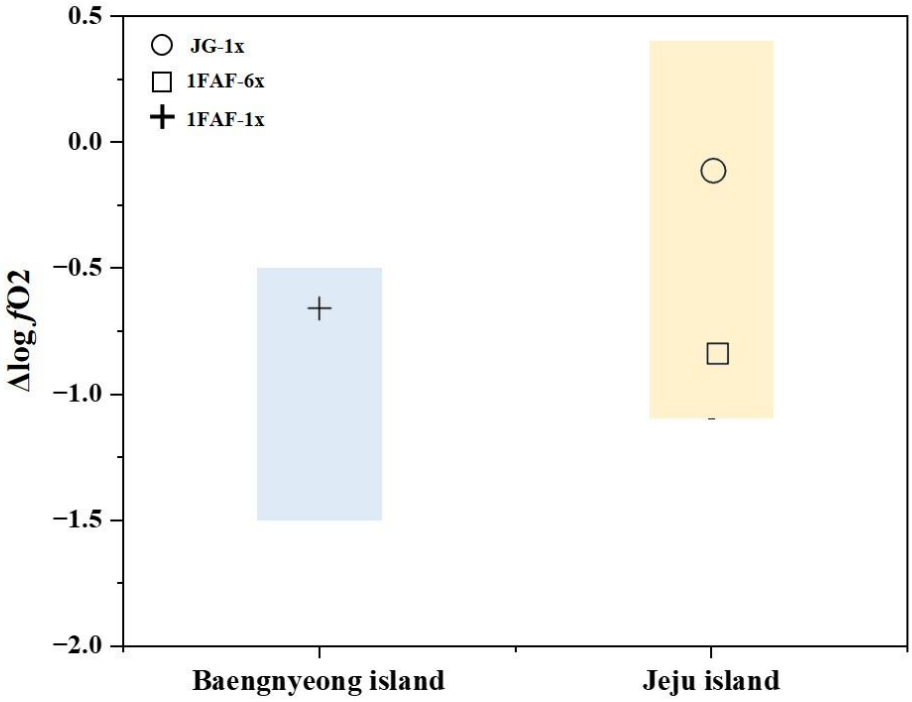
395

396

397

398 **Fig. 7**

399 Comparison of Δ*f*O2 of spinel lherzolites between Jeju and Baengnyeong Islands. The
400 shaded area represents the range reported in previous studies [8, 21, 37, 38].



401